Physics, Chemistry, and Dynamics of Interplanetary Dust
ASP Conference Series, Vol. 104, 1996
Bo A. S. Gustafson and Martha S. Hanner (eds.)

Time Variation of the Solar Dust Cloud

H. Kimura
The Graduate School of Science and Technology, Kobe University, Nada 657, Kobe, Japan

Abstract. We have found from line-of-sight integration of scattered light and thermal emission that the appearance of a hump in the F-corona, which was observed in the near-infrared wavelengths by Peterson (1969) and MacQueen (1968), is very sensitive to the change of size distribution of circumsolar dust grains. Namely, the size distribution affects the balance of scattered sunlight and thermal emission. We suggest that a temporal variation in the size distribution of circumsolar dust grains is a potential origin of the temporal variation of the hump structure observed in the F-corona.

1. Introduction

A temporal variation of the solar dust cloud has been suggested from several observations of the solar F-corona (e.g., Hodapp et al. 1992). An enhancement of the near-infrared brightness at a radial distance of 4 $R_\odot$ (solar radii) from the sun was detected in the 1966 solar eclipse, two months after it, and in the 1983 eclipse (e.g., Peterson 1969; MacQueen 1968; Mizutani et al. 1984), but was undetected in the 1980 and 1991 eclipses (Rao et al. 1981; e.g., Hodapp et al. 1992).

The F-coronal brightness arises from line-of-sight integration of scattered sunlight and thermal emission of circumsolar dust grains. While the scattered light smoothly decreases with increasing solar elongation, the thermal emission shows a peaked feature at the edge of dust-free zone, if the zone exists. Accordingly, when the thermal emission exceeds the scattered light in magnitude, it is possible to detect the sharp peak of thermal emission in the F-coronal brightness. Since the spectrum of the scattered light and thermal emission depend on the size distribution of the grains, we propose that a change in the size distribution affects the near-infrared signature of the F-corona.

According to Hodapp et al. (1992), a direct injection of dust grains into the F-corona by Sun-grazing comets might alter the size distribution of the F-coronal dust. Furthermore, a change in the size distribution might arise from a collision between such cometary grains and the circumsolar dust grains orbiting in the ecliptic plane. In order to examine the hypothesis that the time variation of the humped structure in the solar F-corona results from a change in the size distribution of circumsolar dust grains, we will estimate the near-infrared brightness expected from a fractal dust model using the integration of scattered sunlight and thermal emission along the line of sight.

2. Model of the Solar Dust Cloud

For the model of circumsolar dust grains, we used a fractal aggregate model, i.e., BPCA (Ballistic Particle Cluster Aggregate) from Mukai et al. (1992). Furthermore, we assume that the aggregate consists of silicate and carbon materials. The complex refractive indices and other physical parameters for silicate are cited from Mukai (1990) and Lamy (1974b), respectively. Those for carbon are taken from Hanner (1987) and Mukai & Yamamoto (1979), respectively.

Thermal emission from circumsolar dust grains depends on their temperature as well as their size distribution. The equilibrium temperature of a grain is determined from the energy balance equation (see Lamy 1974b). In comparison with the temperature of a spherical grain, that of a fractal aggregate becomes independent of its radius. Accordingly, fractal aggregates with different radii sublimate at the same solar distance. As a result of this, the solar dust ring of the aggregates, if it exists, will be narrower than that of the spherical grains. Furthermore, the independence of the sublimation zone to the aggregate radius means that the distance to the edge of dust-free zone remains unchanged with changes in the size distribution of the dust.

Knowledge of the spatial density distribution of the grains is necessary for line-of-sight integration of scattered light and thermal emission. In the equilibrium condition for the inward flux of the grains due to the Poynting-Robertson effect, the spatial density distribution $n(r)$ at radial distances in the range of r to $r + dr$ is given by $n(r)r^2dr/dt = \text{const}$. In order to determine dr/dt, we integrate the equation of motion for an aggregate and the mass loss equation due to sublimation simultaneously (see Mukai & Yamamoto 1979). Since it is expected that the eccentricity e of the orbit becomes sufficiently small near the sun due to the Poynting-Robertson effect, we set the initial condition for our calculations to $e = 0$ at a radial distance of 10 $R_\odot$.

The distance to the edge of dust-free zone depends sensitively on the volume fraction of carbon in the composite aggregate. From our numerical simulations of orbital evolution, silicate aggregates containing 0.06 % by volume of carbon sublimate at 4 $R_\odot$, where the peak feature in the near-infrared was observed. The edge of dust-free zone moves from 2.3 $R_\odot$ to 9.4 $R_\odot$ with an increase of carbon content from 0 % to 0.5 %. The silicate aggregates with 0.5-90 % carbon sublimate at about 9 $R_\odot$. When the volume fraction of carbon exceeds 90 %, the distance to the edge of dust-free zone decreases from about 8 $R_\odot$ to 3 $R_\odot$ with increasing carbon content. Mann et al. (1994) have shown similar results from the heliocentric temperature distribution of an aggregate with a 10 μm radius.

The e of the orbit for a spherical grain increases or decreases at the sublimation zone (see Lamy 1974a), whereas that for the aggregate stays in circular motion because the ratio β of the radiation pressure force to the solar gravity on an aggregate becomes independent of its radius. Moreover, the independence of β to the aggregate radius weakens the probability of dynamical stabilization of the aggregate's orbit at the sublimation zone. Consequently, the silicate aggregates containing 0.06 % by volume of carbon concentrate at r =4-4.1 $R_\odot$, a factor of 1.5 relative to the spatial number density expected from the Poynting-Robertson effect alone.

https://doi.org/10.1017/S0252921100501845 Published online by Cambridge University Press

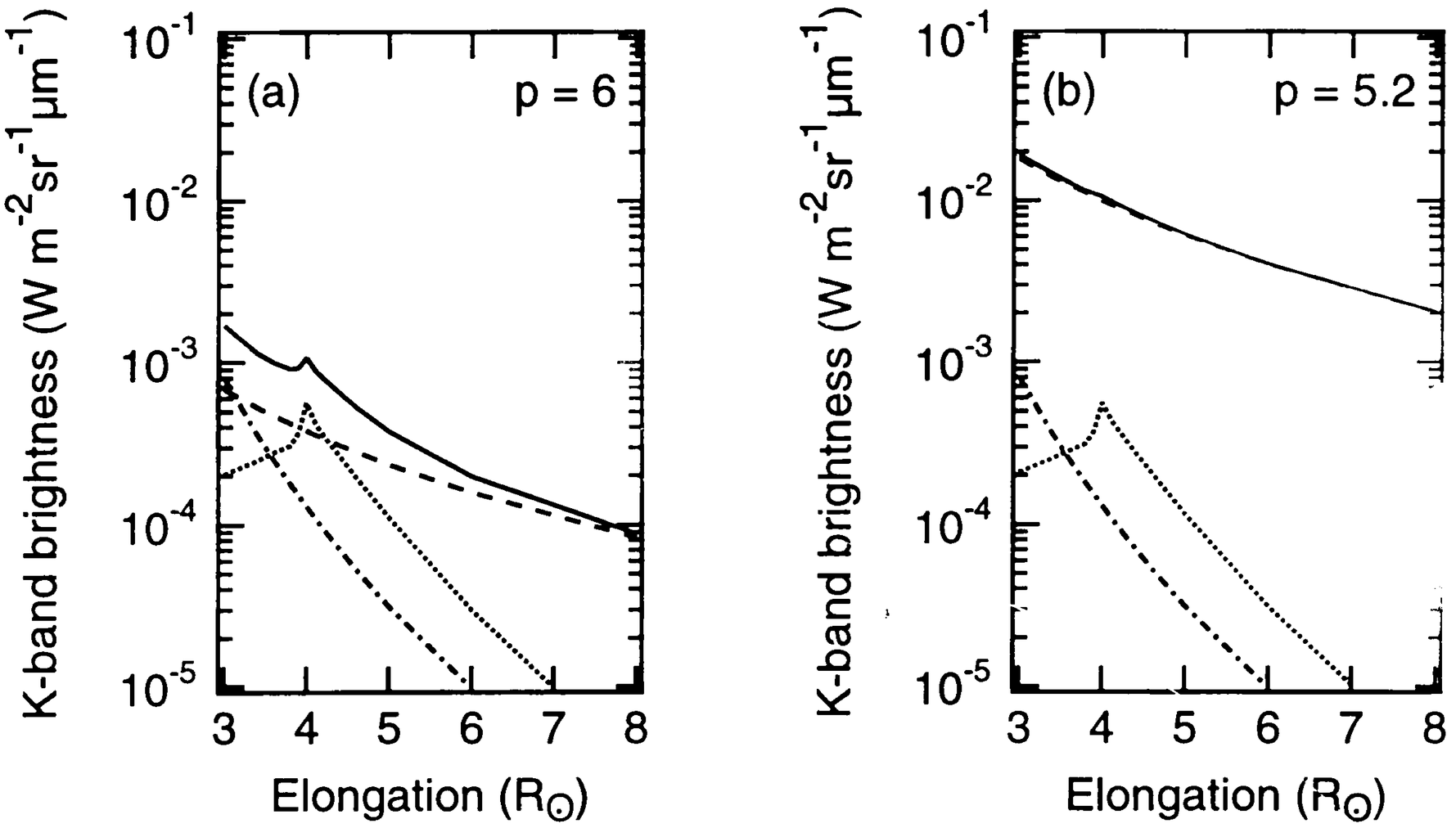

Figure 1. Calculated K-band brightness of the F-corona. Solid line: expected brightness; dotted line: thermal emission; dashed line: scattered light; dash-dotted line: K-corona. (a) The differential size distribution is s^{-p} with $p = 6$ and normalized to the 1967 observation at 5 $R_\odot$. (b) For $p = 5.2$ with the same total number density as in (a) for aggregates in the radius range of 0.01 μm to 1000 μm.

3. Near-infrared Brightness of the Solar Dust Cloud

The brightness of the solar corona contains, in addition to the F-corona, the K-corona due to Thomson scattering of sunlight by electrons (see Mukai et al. 1974). The K-coronal model derived by Newkirk et al. (1970) is used in our calculations. We assume that the differential size distribution for aggregates in the radius range of 0.01 μm to 1000 μm is given by a single power law of the form s^{-p}, where s denotes the characteristic radius of the aggregate defined by Mukai et al. (1992). Furthermore, we assume that the aggregate consists of silicate material containing 0.06 % by volume of carbon, which sublimates at 4 $R_\odot$. Figure 1 shows the calculated brightness of the solar corona in the near-infrared with $p = 6$ (left) and $p = 5.2$ (right). The brightness with the power index $p = 6$ is normalized to the 1967 observation at 5 $R_\odot$. When $p = 6$, the magnitude of the thermal emission exceeds that of the scattered light at 4 $R_\odot$. As a result, the peaked feature of the thermal emission appears in the brightness distribution of the solar corona. On the other hand, the scattered light dominates over thermal emission if $p = 5.2$ at the same total number density. Consequently, the enhancement by thermal emission disappears with the increase of total brightness, as in the 1991 observation of similar brightness magnitude. The total mass density at 1AU is 1.1×10^{-18} kg/m^3 for $p = 5.2$, and 8.3×10^{-19} kg/m^3 for $p = 6$, which is consistent with the value derived by Grün et al. (1985).

https://doi.org/10.1017/S0252921100501845 Published online by Cambridge University Press

4. Discussion

The size distribution of the dust affects the near-infrared signature of the F-coronal brightness remarkably. As shown in Figure 1, the balance between the scattered light and thermal emission strongly depends on the size distribution of the grains. An increase of the power index under the condition of constant total number density at 1AU implies a decrease in the number density of large particles relative to small ones. Since the large particles dominate the scattered light in near-infrared wavelengths (MacQueen & Greeley 1995), the increase of the power index leads to a decrease in scattered light. When the absolute value of the brightness decreases, the enhancement of thermal emission appears in the brightness of the solar corona. As a result, the decrease and increase of large particles relative to small ones leads to the appearance and disappearance, respectively, of the hump structure in the F-coronal brightness. Thus we conclude that the changes in the size distribution of the solar dust cloud produce the temporal variation in the enhancement at 4 $R_{\odot}$ in the F-corona.

Acknowledgments. We would like to thank Professors T. Mukai and R. M. MacQueen for discussions and helpful suggestions to make this paper.

References

Grün, E., Zook, H. A., Fechtig, H., & Giese, R. H. 1985, *Icarus,* **62,** 244

Hanner, M. 1987, in *Infrared Observations of Comets Halley & Wilson and Properties of the Grains,* M. Hanner, NASA Conference Publication xxx, 22

Hodapp, K.-W., MacQueen, R. M., & Hall, D. N. B. 1992, *Nature,* **355,** 707

Lamy, P. L. 1974a, *A&A,* **33,** 191

Lamy, P. L. 1974b, *A&A,* **35,** 197

MacQueen, R. M. 1968, *ApJ,* **154,** 1059

MacQueen, R. M. & Greeley, B. W. 1995, *ApJ,* **440,** 361

Mann, I., Okamoto, H., Mukai, T., Kimura, H., & Kitada, Y. 1994, *A&A,* **291,** 1011

Mizutani, K., Maihara, T., Hiromoto, N., & Takami, H. 1984, *Nature,* **312,** 134

Mukai, T. 1990, in *Evolution of Interstellar Dust and Related Topics,* A. Bonetti, J. M. Greenberg, & S. Aiello, Amsterdam: Elsevier Science, 397

Mukai, T., Ishimoto, H., Kozasa, T., Blum, J., & Greenberg, J. M. 1992, *A&A,* **262,** 315

Mukai, T., & Yamamoto, T. 1979, *Publ. Astron. Soc. Japan,* **31,**585

Mukai, T., Yamamoto, T., Hasegawa, H., Fujiwara, A., & Koike, C. 1974, *Publ. Astron. Soc. Japan,* **26,** 445

Newkirk, Jr., G., Dupree, R. G. & Schmahl, E. J. 1970, *Sol. Phys.,* **15,** 15

Peterson, A. W 1969, *ApJ,* **155,** 1009

Rao, U. R., Alex, T. K., Iyengar, V. S., Kasturirangan, K., Marar, T M. K., Mathur, R. S., & Sharma, D. P. 1981, *Nature,* **289,** 779